



Numerical approximation of free boundary problem arising in electromagnetic shaping

Olivier Coulaud, Olivier Henrot

► **To cite this version:**

Olivier Coulaud, Olivier Henrot. Numerical approximation of free boundary problem arising in electromagnetic shaping. [Research Report] RR-1610, INRIA. 1992, pp.28. <inria-00074950>

HAL Id: inria-00074950

<https://hal.inria.fr/inria-00074950>

Submitted on 24 May 2006

HAL is a multi-disciplinary open access archive for the deposit and dissemination of scientific research documents, whether they are published or not. The documents may come from teaching and research institutions in France or abroad, or from public or private research centers.

L'archive ouverte pluridisciplinaire **HAL**, est destinée au dépôt et à la diffusion de documents scientifiques de niveau recherche, publiés ou non, émanant des établissements d'enseignement et de recherche français ou étrangers, des laboratoires publics ou privés.

INRIA

UNITÉ DE RECHERCHE
INRIA-LORRAINE

Institut National
de Recherche
en Informatique
et en Automatique

Domaine de Voluceau
Rocquencourt
BP 105
78153 Le Chesnay Cedex
France
Tél. (1) 39 63 55 11

Rapports de Recherche

1992



25^{ème}
anniversaire

N° 1610

Programme 6

*Calcul Scientifique, Modélisation et
Logiciel numérique par Ordinateur*

NUMERICAL APPROXIMATION OF A FREE BOUNDARY PROBLEM ARISING IN ELECTROMAGNETIC SHAPING

Olivier COULAUD
Antoine HENROT

Février 1992



★ RR - 1618 ★

Approximation numérique d'un problème à frontière libre issu du formage électromagnétique.

Olivier COULAUD¹ and Antoine HENROT²

February 6, 1992

résumé : On approche numériquement la section d'une colonne de métal liquide plongée dans un champ magnétique extérieur. Le modèle bidimensionnel utilisé nécessite la résolution, par une méthode spectrale d'une équation aux dérivées partielles, avec des conditions non linéaires, posée sur l'extérieur du disque unité pour trouver une transformation conforme convenable. Nous donnons des bornes d'erreur, très précises, pour chacune des étapes du procédé d'approximation. Nous présentons des exemples de formes obtenues à la fois dans le cas du formage extérieur et du formage intérieur.

Numerical Approximation of a Free Boundary Problem Arising in Electromagnetic Shaping.

abstract : We approximate numerically the section of a column of liquid metal submitted to an external electromagnetic field. The bidimensional model used here leads us to solve by a spectral method a nonlinear boundary problem posed on the exterior of the unit disk to find a convenient conformal mapping. We give accurates bound of the errors obtained during our approximation process. We present some examples of shapes for both exterior and interior shaping.

key-words : Free boundary, conformal map, electromagnetic shaping, spectral methods.

AMS-class. : 35R35, 30C30, 65N15, 65N35.

¹INRIA-Lorraine, BP 101, 54600 Villers les NANCY, FRANCE.

²Dép. de Math., Université de Nancy I, URA 750 CNRS, Projet numath.

BP 239, 54506 Vandœuvre les NANCY, FRANCE.

Contents

1	Introduction	3
2	Problem Formulation	3
3	Approximation of problem P_0	6
3.1	Discretisation of problem P_0	7
3.2	Approximation error	9
3.2.1	Approximation for the boundary problem	9
3.2.2	Estimates for the conformal mapping and for the surface	12
4	About interior shaping	15
5	Numerical algorithm	16
5.1	Algorithm for problem P_0	16
5.2	The shaping problem	17
6	Numerical results	19
6.1	The P_0 problem	20
6.2	The shaping problem	22
6.2.1	The exterior shaping	22
6.2.2	The interior shaping	26
	References	28

1 Introduction

We study here a free boundary problem arising in electromagnetic shaping. The bidimensional model leads us to use conformal mappings to transform the problem into a problem posed on the exterior of the unit disk. We compute the conformal mapping by solving a nonlinear problem P_0 and the solution of the electromagnetic shaping problem is reached by a fixed point method. In part 3, we study more deeply the approximation scheme based on a Galerkin spectral method to solve the nonlinear boundary value problem. First, all the approximation results presented in [4] are extended, then we give an accurate bound for the error in L^∞ norm for the conformal mappings and the surfaces. In part 4 we give some comments about the so-called "interior shaping" and we explain how it can be obtained by few modifications of the previous one. We describe in part 5 the numerical algorithm employed to solve the P_0 problem and the algorithm to reach the wanted configuration based on the secant method. In part 6, we show that our solver is very efficient for P_0 problem, then different configurations of exterior shaping are investigated. We also present the evolution of the shape when τ tends to 0. Finally, we present some results for the interior shaping.

2 Problem Formulation

We consider a vertical column of molten liquid falling down in an horizontal electromagnetic field created by vertical conductors. The frequency of the imposed current is assumed to be so high that the field doesn't penetrate into the liquid. Due to the action of the magnetic field the column of metal liquid is shaped. Because of the great height of this column, we can consider the two-dimensional model introduced in [2], [10], based on an horizontal section of the molten liquid.

We denote by Ω the exterior domain of the liquid, Γ its boundary and by $\mathbf{j}_0 = (0, 0, j_0)$ the current density vector. The total magnetic field \mathbf{B} is governed by Maxwell's equations

which we express as

$$\begin{cases} \operatorname{rot} \mathbf{B} = \mu_0 \mathbf{j}_0 & \text{in } \Omega \\ \operatorname{div} \mathbf{B} = 0 & \text{in } \Omega \\ \mathbf{B} \cdot \mathbf{n} = 0 & \text{on } \Gamma \\ \lim_{|z|_2 \rightarrow \infty} |\mathbf{B}|_2 = 0 \end{cases} \quad (2-1)$$

where μ_0 is the permeability of vacuum, \mathbf{n} the exterior unit normal vector of Γ , $|\cdot|_2$ the euclidian norm.

Moreover on the free boundary Γ the following Bernoulli equilibria equation is satisfied

$$\frac{|\mathbf{B}|_2^2}{2\mu_0} + \sigma \mathcal{C} = \text{constant} \quad (2-2)$$

where \mathcal{C} is the curvature of Γ and σ the surface tension of the liquid. The constant in (2-2) is unknown.

Let us consider here the following free boundary problem. The current density \mathbf{j}_0 is given and the problem is to find the shape Ω and the magnetic field \mathbf{B} such that (2-1) and (2-2) are satisfied. According to [10], we assume now that the boundary Γ of Ω solution of (2-1)-(2-2) is a closed Jordan curve. Then, the domain Ω is the image by a conformal mapping Φ of the exterior of the unit disk Ω_0 . It is easy to see ([10]) that v given by

$$v(z) = \ln(|\Phi'(z)|) \quad \text{with } z = x + iy \quad (2-3)$$

is solution of

$$\begin{cases} \Delta v = 0 & \text{in } \Omega_0 \\ \tau \frac{\partial v}{\partial \mathbf{n}} = g^2 e^{-v} - p e^v + \tau & \text{on } \Gamma_0 \\ v \text{ bounded at infinity} \end{cases} \quad (2-4)$$

where Γ_0 is the unit circle, $\tau = 2\sigma\mu_0$, p is the constant appearing in (2-2) multiplied by $2\mu_0$ and

$$g^2 = g^2(\theta) := (p - \tau\mathcal{C})|\Phi'(e^{i\theta})|^2.$$

Henrot and Pierre have shown in [11], that the function g can be expressed only in term of $J_0 = j_0 \circ \Phi$, the image of j_0 under Φ^{-1} . In the case of m linear vertical conductors, for instance, j_0 is given by

$$j_0 = \sum_{k=1}^m \alpha_k \delta_{Z_k} \quad \text{with } \alpha_k \in \mathbb{R}, Z_k \in \Omega \quad (2-5)$$

and g is given by

$$g(\theta) = \sum_{k=1}^m -\frac{\alpha_k \mu_0}{2\pi} \left\{ \frac{e^{i\theta}}{z_k - e^{i\theta}} + \frac{e^{-i\theta}}{\bar{z}_k - e^{-i\theta}} + 1 \right\} \quad (2-6)$$

where δ_{Z_k} is the Dirac mass at Z_k , Z_k is the position of the k^{th} conductor, α_k its strength and $z_k = \Phi^{-1}(Z_k)$ for $k = 1, \dots, m$.

Now let us explain the procedure to obtain the free boundary Γ . Our problem is to determine the conformal mapping Φ through the function v solution of (2-4). The knowledge of g by (2-6) is implicit since it depends on Φ . So, we must use a fixed point method.

Let $\mathbb{X} = \mathbb{R}_*^+ \times \{(z_1, \dots, z_m) \in \mathbb{C}^m, |z_i| > 1, i = 1, \dots, m\}$, we introduce the function F defined by

$$F : \mathbb{X} \longrightarrow \mathbb{R}_*^+ \times \mathbb{C}^m$$

$$x = (p, z_1, \dots, z_m) \longmapsto F(x) = (S, \Phi(z_1), \dots, \Phi(z_m)) \quad (2-7)$$

where S is the surface of Ω^c (the molten liquid). Notice, for the following, that S can be computed by

$$S := \frac{1}{2} \Re \left\{ \int_0^{2\pi} e^{i\theta} \Phi'(e^{i\theta}) \bar{\Phi}(e^{i\theta}) d\theta \right\}. \quad (2-8)$$

For each x given in \mathbb{X} , $F(x)$ is evaluated by the following algorithm called problem P_0 .

$$(P_0) \left\{ \begin{array}{l} \text{Let } g \text{ be given by (2-6) and } p \in \mathbb{R}_*^+ \\ \bullet \text{ We find } v(re^{i\theta}) = \sum_{k=-\infty}^{+\infty} a_k e^{ik\theta} r^{-|k|} \text{ solution of (2-4).} \\ \bullet \text{ We construct the holomorphic function } V, \text{ defined on } \Omega_0, \\ \quad \text{such that } : v(z) = \Re \text{al}(V(z)). \\ \bullet \text{ We deduce } \Phi'(z) = \omega e^{V(z)} \quad \text{for } |z| \geq 1 \text{ and } |\omega| = 1. \\ \bullet \text{ We integrate if possible to obtain } \Phi(z). \end{array} \right.$$

Then we are able to compute $F(x) = (S, \Phi(z_1), \dots, \Phi(z_m))$.

Unfortunately the last step of this algorithm is not always possible due to the fact that Ω_0 is not simply connected. We have seen in [11] that the condition for Φ to exist is

$$\int_0^{2\pi} v(e^{i\theta}) e^{i\theta} d\theta = 0. \quad (2-9)$$

So the set of x in \mathbb{X} for which this condition is realized turns out to be a regular manifold, say \mathcal{D} , of $\mathbb{R}_*^+ \times \Omega_0^m$ of complex codimension one (see [7]). Nevertheless, if the original

distribution of masses (Z_k, α_k) presents some good symmetry property (invariance by a rotation of angle $2\pi/q$ for instance) we can take into account this property for the z_k 's and then, the condition (2-9) turns out to be automatically satisfied. To avoid complications, we shall always consider such a symmetry property in the following.

The last difficulty which can appear with this "implicit approach" is the fact that the holomorphic function Φ obtained by this way may not be univalent. If it is the case, the solution is not admissible since Φ must be a conformal mapping. We have shown in [8], that the univalence of Φ on Ω_0 was equivalent to univalence of Φ on Γ_0 . So we have to introduce a test to decide whether the curve $\Gamma = \Phi(\Gamma_0)$ has double points or not. Notice finally that the set of x such that Φ is defined and univalent on Ω_0 is an open subset of the manifold \mathcal{D} . We will denote it by \mathbb{H} in the following.

Let the conductors $(Z_1, \alpha_1), \dots, (Z_m, \alpha_m)$ be given, the direct problem is to obtain a shape of the liquid with a given surface S_0 . The solution of this problem is obtained when we can solve the nonlinear equation

$$\text{find } x \in \mathbb{H} \text{ such that } F(x) = (S_0, Z_1, \dots, Z_m). \quad (2-10)$$

3 Approximation of problem P_0

Throughout this section we assume that the function g and the real p are given. To determine v , we transform (2-4) into a boundary problem posed on Γ_0 . This one will be solved by a Galerkin spectral method (see [4]).

We denote by $\mathcal{C}(\Gamma_0)$ the space of continuous functions on Γ_0 , by $\mathcal{C}_b(\overline{\Omega}_0)$ the space of bounded continuous functions on $\overline{\Omega}_0$ and by $\mathcal{C}_n^1(\overline{\Omega}_0)$ the space of functions v in $\mathcal{C}_b(\overline{\Omega}_0)$ such that the normal derivative $\frac{\partial v}{\partial n}$ is defined and continuous on Γ_0 .

For $\varphi \in \mathcal{C}(\Gamma_0)$, we denote by $u_e(\varphi)$ the unique solution of the exterior Dirichlet problem

$$\left\{ \begin{array}{ll} \text{find } u \in \mathcal{C}_b(\overline{\Omega}_0) \text{ such that} & \\ \Delta u = 0 & \text{in } \Omega_0 \\ u = \varphi & \text{on } \Gamma_0. \end{array} \right. \quad (3-1)$$

Then, we define the exterior capacity operator C_e by

$$\begin{cases} D(C_e) = \{\varphi \in \mathcal{C}(\Gamma_0); u_e(\varphi) \in \mathcal{C}_n^1(\bar{\Omega}_0)\} \\ C_e\varphi = \frac{\partial}{\partial n}u_e(\varphi) \end{cases} \quad (3-2)$$

(see [5] for more details). With these definitions, problem (2-4) is equivalent to

$$\begin{cases} \text{find } \varphi \in D(C_e) \text{ such that} \\ \tau C_e\varphi + \beta(\theta, \varphi(\theta)) = \tau \quad \text{on } \Gamma_0 \\ \text{then } v := u_e(\varphi) \end{cases} \quad (3-3)$$

where $\beta(\theta, \varphi) = pe^\varphi - g^2(\theta)e^{-\varphi} \quad \forall \theta \in \Gamma_0$.

We know ([11]), that (3-3) has a unique solution. Moreover if g^2 is analytic then v is analytic on $\bar{\Omega}_0$ (up to the boundary).

3.1 Discretisation of problem P_0

We denote, as usual, by P_N the space of trigonometric polynomials whose degree does not exceed N , defined by :

$$P_N := \text{span} \{ \varphi_k = e^{ik\theta}; \theta \in [0, 2\pi[; -N \leq k \leq N \}$$

and by Π_N the orthogonal projection operator defined from $L^2(\Gamma_0)$ into P_N by :

$$\forall v \in L^2(\Gamma_0) \quad \langle v - \Pi_N v, \varphi \rangle = 0 \quad \forall \varphi \in P_N \quad (3-4)$$

where $\langle u, v \rangle = \frac{1}{2\pi} \int_0^{2\pi} u(\theta)\bar{v}(\theta)d\theta$ denotes the inner product on $L^2(\Gamma_0)$ and $\|\cdot\|$ the associated norm.

We will use the space of periodic function $H_{per}^s(\Gamma_0)$ which can be defined, for instance by

$$H_{per}^s(\Gamma_0) = \left\{ \varphi \in L^2(\Gamma_0), \varphi \text{ periodic, } \varphi = \sum_{n=-\infty}^{+\infty} a_n \varphi_n \text{ such that} \right. \\ \left. \sum_{n=-\infty}^{+\infty} (1+n^2)^s |a_n|^2 < +\infty \right\} \quad (3-5)$$

equipped with the usual norms $\|\cdot\|_s$ (see [1] and [3] for more details on spectral approximation). The use of spectral method to solve (3-3), as introduced in [4], is justified by the following properties :

1) Every bounded harmonic function v defined on Ω_0 can be expanded as :

$$v(z) = \sum_{k=-\infty}^{+\infty} a_k \psi_k(z) \quad \text{where } \psi_k(z) = r^{-|k|} \varphi_k(\theta) \quad \text{with } z = r e^{i\theta}. \quad (3-6)$$

2) Commutativity of the operator C_e with operator Π_N . Indeed we have

$$C_e \varphi_k = |k| \varphi_k. \quad (3-7)$$

Let us remark that

$$\frac{\partial \beta}{\partial \varphi} = p e^\varphi + g^2 e^{-\varphi} \geq 2\sqrt{p}|g|.$$

So there exists a regular positive function λ , $\lambda \neq 0$, such that

$$\frac{\partial \beta}{\partial \varphi} \geq \lambda(\theta) \quad \forall \theta \in [0, 2\pi[. \quad (3-8)$$

This ensures that problem (3-3) is well posed. The best choice of λ , see [4], is

$$\lambda(\theta) = \begin{cases} 2\sqrt{p} g_{min} & \text{if } g_{min} > 0 \\ 2\sqrt{p} g^2(\theta)/g_{max} & \text{if } g_{min} = 0 \end{cases} \quad (3-9)$$

where $g_{max} = \max_{\theta \in [0, 2\pi[} |g(\theta)|$ and $g_{min} = \min_{\theta \in [0, 2\pi[} |g(\theta)|$.

Let $\gamma(\theta, \varphi) = \beta(\theta, \varphi) - \lambda(\theta)\varphi$; according to (3-8), γ is monotone in φ . Under these conditions we can use all results appearing in [4] and [11].

Problem (3-3) is written in P_N , as

$$\begin{cases} \text{Find } \varphi^N \in P_N, \varphi^N \text{ real, such that} \\ \delta \varphi^N + \Pi_N(\lambda_N \varphi^N) + \tau C_e \varphi^N = \tau - \Pi_N(\beta(\cdot, \varphi^N) - \lambda_N \varphi^N) + \delta \varphi^N \end{cases} \quad (3-10)$$

where $\lambda_N = \Pi_N \lambda$ and δ is a relaxation parameter.

We solve (3-10) with a Galerkin method and a fixed point scheme, and we obtain $(a_k)_{k=-N}^N$ the spectral coefficients of φ^N with $a_{-k} = \bar{a}_k$. Let us consider v_N the harmonic function in Ω_0 with $v_N = \varphi^N$ on Γ_0 , then v_N has the following expansion

$$v_N(z) = \sum_{k=-N}^N a_k \psi_k(z) \quad \forall z \in \Omega_0. \quad (3-11)$$

We construct now, the holomorphic function V_N , defined on Ω_0 , such that $v_N = \Real(V_N)$.

We have

$$V_N(z) = v_N(z) + i w_N(z) = a_0 + 2 \sum_{k=1}^N a_{-k} z^{-k} \quad \forall z \in \Omega_0. \quad (3-12)$$

Notice that $a_{-1} = 0$ if and only if (2-9) is satisfied. Finally we deduce $\Phi'_N(z) = e^{V_N(z)}$, and by integration $\Phi_N(z)$ for all z in Ω_0 . The surface S_N being computed by

$$S_N := \frac{1}{2} \Real \left\{ \int_0^{2\pi} e^{i\theta} \Phi'_N(e^{i\theta}) \bar{\Phi}_N(e^{i\theta}) d\theta \right\}. \quad (3-13)$$

3.2 Approximation error

3.2.1 Approximation for the boundary problem

We have established in [4] for the Galerkin spectral approximation of (3-10) the following result.

Theorem 3.1 *Let φ^* be the solution of (3-3) and φ^N the solution of (3-10). There exists a constant C depending only on λ, β and φ^* such that*

$$\|\varphi^N - \varphi^*\| \leq C(\|\lambda - \Pi_N \lambda\| + \|\varphi^* - \Pi_N \varphi^*\|)$$

We can here, slightly improve this result, working with the $H^{\frac{1}{2}}$ norm.

Theorem 3.2 *Under the assumptions of theorem 3.1, there exists a constant C depending only on λ, β , and φ^* such that*

$$\|\varphi^N - \varphi^*\|_{\frac{1}{2}} \leq C(\|\lambda - \Pi_N \lambda\| + \|\varphi^* - \Pi_N \varphi^*\|_{\frac{1}{2}})$$

Proof.

We follow the demonstration of theorem 3.1, so, for more details, we refer to [4]. By (3-10) φ^N is solution of :

$$\langle (\lambda_N I + \tau C_e) \varphi^N + \gamma(\cdot, \Pi_N \varphi^N), \varphi_k \rangle = \langle \tau, \varphi_k \rangle \quad -N \leq k \leq N. \quad (3-14)$$

Let us introduce φ^* the solution of (3-3) ; then $\Pi_N \varphi^*$ verifies

$$\begin{aligned} \langle (\lambda_N I + \tau C_e) \Pi_N \varphi^* + \gamma(\cdot, \Pi_N \varphi^*), \varphi_k \rangle = \\ \langle \tau + \lambda_N \Pi_N \varphi^* - \lambda \varphi^* + \gamma(\cdot, \Pi_N \varphi^*) - \gamma(\cdot, \varphi^*), \varphi_k \rangle \quad -N \leq k \leq N \end{aligned} \quad (3-15)$$

Let us set $e_N = \Pi_N \varphi^* - \varphi^N$ subtracting (3-14) from (3-15) we obtain for all $k \in [-N, N]$

$$\begin{aligned} \langle (\lambda_N I + \tau C_e) e_N + \gamma(\cdot, \Pi_N \varphi^*) - \gamma(\cdot, \varphi^N), \varphi_k \rangle = \\ \langle \lambda_N \Pi_N \varphi^* - \lambda \varphi^* + \gamma(\cdot, \Pi_N \varphi^*) - \gamma(\cdot, \varphi^*), \varphi_k \rangle. \end{aligned} \quad (3-16)$$

Multiplying (3-16) by the spectral coefficients of e_N and adding up from $-N$ to N yields

$$\begin{aligned} \int_{\Gamma_0} \lambda_N |e_N|^2 + \tau \int_{\Gamma_0} C_e e_N \bar{e}_N + \int_{\Gamma_0} (\gamma(\cdot, \Pi_N \varphi^*) - \gamma(\cdot, \varphi^N)) \bar{e}_N \\ = \langle \lambda_N \Pi_N \varphi^* - \lambda \varphi^* + \gamma(\cdot, \Pi_N \varphi^*) - \gamma(\cdot, \varphi^*), e_N \rangle \end{aligned}$$

Using monotonicity of the function γ yields

$$\int_{\Gamma_0} \lambda_N |e_N|^2 + \tau \int_{\Gamma_0} C_e e_N \bar{e}_N \leq \langle (\lambda_N - \lambda) \Pi_N \varphi^*, e_N \rangle + \langle \beta(\cdot, \Pi_N \varphi^*) - \beta(\cdot, \varphi^*), e_N \rangle.$$

We introduce now the operator Q_N defined by $Q_N = I - \Pi_N$. Since φ^* is (at least !) C^1 on Γ_0 , we have $\|\Pi_N \varphi^*\|_\infty < C_1$, C_1 independent of N , and then using the fact that β is Lipschitz with respect to its second argument with C_2 as Lipschitz constant and the Cauchy-Schwarz inequality we obtain

$$\int_{\Gamma_0} \lambda_N |e_N|^2 + \tau \int_{\Gamma_0} C_e e_N \bar{e}_N \leq (C_1 \|Q_N \lambda\| + C_2 \|Q_N \varphi^*\|) \|e_N\|.$$

Let us remark that if $e_N = \sum_{k=-N}^N a_k \varphi_k$ we have

$$\int_{\Gamma_0} C_e e_N \bar{e}_N = \sum_{k=-N}^N |k| |a_k|^2$$

which is nearly but not $\|e_N\|_{\frac{1}{2}}^2$. Therefore we need to use the following lemma to obtain $\|e_N\|_{\frac{1}{2}}$.

Lemma 3.1 (see [4]) *For every $\lambda \in C(\Gamma_0)$, $\lambda \geq 0$, $\lambda \not\equiv 0 \exists C_0$, (which depends only on λ) such that*

$$\forall v \in H_{loc}^1(\bar{\Omega}_0) \quad C_0 \int_{\Gamma_0} v^2 \leq \int_{\Gamma_0} \lambda v^2 + \int_{\Omega_0} |\nabla v|^2.$$

It follows from definition of operator C_e that $\int_{\Gamma_0} C_e v_N \bar{v}_N = \int_{\Omega_0} |\nabla v_N|^2$.

We write now $\lambda_N = \lambda - Q_N \lambda$ then

$$\int_{\Gamma_0} \lambda_N |e_N|^2 + \tau \int_{\Gamma_0} C_e e_N \bar{e}_N = \int_{\Gamma_0} \lambda |e_N|^2 + \tau \int_{\Gamma_0} C_e e_N \bar{e}_N - \int_{\Gamma_0} Q_N \lambda |e_N|^2.$$

Lemma 3.1 and the uniform majoration of $Q_N \lambda$ imply

$$\int_{\Gamma_0} \lambda_N |e_N|^2 + \tau \int_{\Gamma_0} C_e e_N \bar{e}_N \geq \left(\frac{\tau C_0}{2} - \|Q_N \lambda\|_\infty \right) \|e_N\|^2 + \frac{\tau}{2} \int_{\Gamma_0} C_e e_N \bar{e}_N.$$

Due to the regularity of λ we can choose N_0 such that $\forall N \geq N_0$ we have $\|Q_N \lambda\|_\infty \leq \frac{\tau C_0}{4}$, see [3], so we have

$$\frac{\tau C_0}{4} \|e_N\|^2 + \frac{\tau}{2} \int_{\Gamma_0} C_e e_N \bar{e}_N \leq (C_1 \|Q_N \lambda\| + C_2 \|Q_N \varphi^*\|) \|e_N\|$$

$$\frac{\tau}{2} \inf\left(1, \frac{C_0}{2}\right) \left(\|e_N\|^2 + \int_{\Gamma_0} C_e e_N \bar{e}_N \right) \leq \max(C_1, C_2) (\|Q_N \lambda\| + \|Q_N \varphi^*\|) \|e_N\|.$$

Let us remark that

$$\|e_N\|^2 + \int_{\Gamma_0} C_r e_N \bar{e}_N = \sum_{k=-N}^N (1 + |k|) |a_k|^2 \geq \sum_{k=-N}^N (1 + |k|^2)^{\frac{1}{2}} |a_k|^2 = \|e_N\|_{\frac{1}{2}}^2$$

then we finally obtain

$$\|e_N\|_{\frac{1}{2}} \leq C \{ \|Q_N \lambda\| + \|Q_N \varphi^*\| \}, \quad \text{since } \|e_N\| \leq \|e_N\|_{\frac{1}{2}}.$$

Whence the $H^{\frac{1}{2}}(\Gamma_0)$ inequality of theorem 3.2 using

$$\|\varphi^N - \varphi^*\|_{\frac{1}{2}} \leq \|Q_N \varphi^*\|_{\frac{1}{2}} + \|e_N\|_{\frac{1}{2}}. \quad \square$$

Proposition 3.1 *Under the assumptions of theorem 3.1, there exists a constant C such that*

$$\|\varphi^N - \varphi^*\|_s \leq \|\varphi^* - \Pi_N \varphi^*\|_s + CN^s \{ \|\varphi^* - \Pi_N \varphi^*\| + \|\lambda - \Pi_N \lambda\| \} \quad \forall s \geq 1.$$

Proof.

To obtain this inequality, we estimate directly the H^s norm by the L^2 norm. Triangle inequality gives

$$\|\varphi^N - \varphi^*\|_s \leq \|Q_N \varphi^*\|_s + \|e_N\|_s.$$

Now, if $e_N = \varphi^N - \Pi_N \varphi^* = \sum_{k=-N}^N \hat{e}_k \varphi_k$ then

$$\|\varphi^N - \Pi_N \varphi^*\|_s^2 = \|e_N\|_s^2 = \sum_{k=-N}^N (1 + k^2)^s |\hat{e}_k|^2.$$

Taking into account that $1 + k^2 \leq 2N^2$, we obtain

$$\|\varphi^N - \Pi_N \varphi^*\|_s^2 \leq 2^s N^{2s} \sum_{k=-N}^N |\hat{e}_k|^2,$$

and then

$$\|\varphi^N - \Pi_N \varphi^*\|_s \leq CN^s \|\varphi^N - \Pi_N \varphi^*\|$$

whence the proposition. \square

If g^2 is analytic we know (see [11]) that v is analytic on $\bar{\Omega}_0$ then φ^* is analytic and so is λ by construction. Assume that

$$-\eta \leq \text{Im} z \leq \eta \tag{3-17}$$

is a strip of analyticity where both $g^2(z)$ and $\varphi^*(z)$ have an absolutely convergent expansion.

Corollary 3.1 *For any η satisfying (3-17) and for N large enough we have*

$$\|\varphi^N - \varphi^*\|_s \leq C(\eta)N^s e^{-\eta N} \quad \text{for any } s \text{ in } s \geq 1.$$

The proof follows from estimation of $\|w - \Pi_N w\|_s$, since when w is 2π -periodic analytic we have $\|w - \Pi w\|_s \leq C(\eta)N^s e^{-\eta N}$, see [14].

3.2.2 Estimates for the conformal mapping and for the surface

Let us introduce D a ring in Ω_0 which contains all the conductors z_i . We denote by Φ (resp. Φ_N) the conformal mapping constructed from v (resp v_N) as introduced in the problem formulation.

Theorem 3.3 *Under the hypothesis of corollary 3.1 there exist two constants C_1, C_2 , depending only on D, g and φ^* such that*

$$\begin{aligned} |\Phi - \Phi_N|_{L^\infty(\bar{D})} &\leq C_1 N^{\frac{1}{2}} e^{-\eta N} \\ |S - S_N| &\leq C_2 N^{\frac{3}{2}} e^{-\eta N}. \end{aligned}$$

The two conformal mappings Φ and Φ_N are defined by

$$\Phi(z) = \Phi(1) + \int_{\gamma_z} \Phi'(\xi) d\xi$$

and

$$\Phi_N(z) = \Phi_N(1) + \int_{\gamma_z} \Phi'_N(\xi) d\xi$$

where γ_z is an integration path connecting the point 1 to z . We can choose the same constant of integration i.e. $\Phi_N(1) = \Phi(1)$.

To prove this theorem, the knowledge of all approximation errors during the process of construction of Φ' are needed.

Lemma 3.2 *Under the hypothesis of theorem 3.3, there exists $C = C(\eta)$ such that*

$$\begin{aligned} \|v - v_N\|_{H^1(D)} &\leq CN^{\frac{1}{2}} e^{-\eta N} \\ \|v - v_N\|_{L^\infty(D)} &\leq CN^{\frac{3}{2}} e^{-\eta N} \end{aligned}$$

where v is the solution of (3-3) and v_N is given by (3-11).

Proof.

It is classical that for the exterior Dirichlet problem

$$\begin{cases} \Delta u = 0 & \text{in } \Omega_0 \\ u = \varphi & \text{on } \Gamma_0 \\ u \text{ bounded at infinity,} \end{cases} \quad (3-18)$$

the map $\varphi \mapsto u$ is continuous from $H^{\frac{1}{2}}(\Gamma_0)$ into $H_{loc}^1(\Omega_0)$ and from $H^{\frac{3}{2}}(\Gamma_0)$ into $H_{loc}^2(\Omega_0)$, that is to say, there exist constants C depending only on the ring D such that

$$\|u\|_{H^1(D)} \leq C\|\varphi\|_{\frac{1}{2}} \quad \text{and} \quad \|u\|_{H^2(D)} \leq C\|\varphi\|_{\frac{3}{2}}.$$

Lemma 3.2 follows immediately using corollary 3.1 and Sobolev embedding for the L^∞ norm. \square

Lemma 3.3 *Let V be given by P_0 and V_N by (3-12). We have*

$$\begin{aligned} \|V - V_N\|_{H^1(D)} &\leq C\|\varphi^* - \varphi^N\|_{\frac{1}{2}} \leq CN^{\frac{1}{2}}e^{-\eta N} \\ \|V - V_N\|_{L^\infty(D)} &\leq C\|\varphi^* - \varphi^N\|_{\frac{3}{2}} \leq CN^{\frac{3}{2}}e^{-\eta N}. \end{aligned}$$

Proof.

We have to estimate the real part and the imaginary part of $V - V_N$.

Let $V = v + i w$ and $V_N = v_N + i w_N$. The Cauchy formula gives

$$V' - V'_N = \frac{\partial}{\partial x}(v - v_N) - i \frac{\partial}{\partial y}(v - v_N),$$

and then, according to lemma 3-2, to prove lemma 3-3 it is sufficient to estimate $w - w_N$ in $L^2(D)$ norm.

Now the construction of V and V_N gives $w = \sum_{n=-\infty}^{+\infty} b_n \psi_n$ and $w_N = \sum_{n=-N}^N d_n \psi_n$ with

$$b_n = \begin{cases} i\bar{a}_n & \text{if } n \leq -1 \\ \frac{a_0 - \bar{a}_0}{2i} & \text{if } n = 0 \\ -ia_{-n} & \text{if } n \geq 1 \end{cases} \quad d_n = \begin{cases} i\bar{a}_n & \text{if } n \leq -1 \\ \frac{\bar{a}_0 - a_0}{2i} & \text{if } n = 0 \\ -i\tilde{a}_{-n} & \text{if } n \geq 1 \end{cases}$$

where a_n and \tilde{a}_n are the spectral coefficients of φ and φ^N .

Since the coefficients of the expansion of $w - w_N$ are similar to those of $v - v_N$, the result is given by lemma 3.2. \square

Now we can start the proof of theorem 3.3. For $z \in D$ we have

$$\Phi(z) - \Phi_N(z) = \int_{\gamma_z} (\Phi'(\xi) - \Phi'_N(\xi)) d\xi$$

now

$$\Phi'(\xi) - \Phi'_N(\xi) = e^{V(z)} - e^{V_N(z)}.$$

Using the mean-value theorem and lemma 3.3, we obtain :

$$|\Phi'(\xi) - \Phi'_N(\xi)| \leq e^{3\|v\|_\infty} |V(\xi) - V_N(\xi)| \quad (3-19)$$

so

$$|\Phi(z) - \Phi_N(z)| \leq e^{3\|v\|_\infty} \int_{\gamma_z} |V(\xi) - V_N(\xi)| |d\xi|$$

and the Cauchy-Schwarz inequality gives

$$|\Phi(z) - \Phi_N(z)| \leq C(\|v\|_\infty) |\gamma_z|^{\frac{1}{2}} \|V - V_N\|_{L^2(\gamma_z)}$$

where $|\gamma_z|$ is the length of the path γ_z . By the trace theorem we have

$$|\Phi(z) - \Phi_N(z)| \leq C(\|v\|_\infty) |\gamma_z|^{\frac{1}{2}} \|V - V_N\|_{H^1(D)}.$$

We denote by $L = \sup_{z \in D} |\gamma_z|^{\frac{1}{2}}$. We can obviously choose γ_z for all $z \in D$, such that $L < \infty$.

By using lemma 3.3 we obtain that

$$|\Phi(z) - \Phi_N(z)| \leq C(\|v\|_\infty) L N^{\frac{1}{2}} e^{-\eta N} \quad \forall z \in D$$

which gives the first inequality of theorem 3.3.

Now we must estimate the error between the exact surface S and the approximate one. These surfaces are computed by $S = \Re\text{al}(I)$ and $S_N = \Re\text{al}(I_N)$ where

$$I = \frac{1}{2} \left\{ \int_0^{2\pi} e^{i\theta} \Phi'(e^{i\theta}) \overline{\Phi}(e^{i\theta}) d\theta \right\}$$

and

$$I_N = \frac{1}{2} \left\{ \int_0^{2\pi} e^{i\theta} \Phi'_N(e^{i\theta}) \overline{\Phi}_N(e^{i\theta}) d\theta \right\}.$$

With the help of the scalar product of $L^2(\Gamma_0)$, we can rewrite I and I_N as follows

$$I = \pi \langle e^{i\theta} \Phi'(e^{i\theta}), \Phi(e^{i\theta}) \rangle$$

and

$$I_N = \pi \langle e^{i\theta} \Phi'_N(e^{i\theta}), \Phi_N(e^{i\theta}) \rangle .$$

Then

$$\begin{aligned} I - I_N = \pi \langle e^{i\theta} (\Phi'(e^{i\theta}) - \Phi'_N(e^{i\theta})) , \Phi(e^{i\theta}) \rangle \\ + \pi \langle e^{i\theta} \Phi'_N(e^{i\theta}), \Phi(e^{i\theta}) - \Phi_N(e^{i\theta}) \rangle . \end{aligned}$$

Using Cauchy-Schwarz inequality yields

$$|I - I_N| \leq C \|\Phi' - \Phi'_N\| \|\Phi\| + C \|\Phi'_N\| \|\Phi - \Phi_N\|.$$

Inequality (3-19) implies

$$|\Phi'(z) - \Phi'_N(z)| \leq C(\|v\|_\infty) |V(z) - V_N(z)| \quad \forall z \in D. \quad (3-20)$$

Now for N large enough lemma 3.3 gives $|\Phi'_N(z)| \leq 1 + |\Phi'(z)|$, then

$$|I - I_N| \leq C(\|\Phi\|, \|\Phi'\|, \|v\|_\infty) \{ \|V - V_N\| + \|\Phi - \Phi_N\| \} .$$

We estimate each $L^2(\Gamma_0)$ norm by the $L^\infty(D)$ norm and we use the first estimation of theorem 3.3 and inequality (3-17) to obtain

$$|I - I_N| \leq C(\Phi, \Phi', V) \{ \|V - V_N\|_{L^\infty(D)} + \|\Phi - \Phi_N\|_{L^\infty(D)} \} .$$

Then the result follows from lemma 3.3 and the first estimation of theorem 3.3. \square

4 About interior shaping

The case of interior shaping, where the conductors are introduced inside the liquid metal can be studied by the same approach. Here we have to find the shape taken by the metal around the conductors.

Now the domain Ω is bounded and we have to work with the unit disk Ω_1 , instead of the exterior of the unit disk, to find the conformal map from Ω_1 into Ω .

In fact we have nearly the same problem to solve. The conformal map is given by (2-3) where v is an harmonic function in Ω_1 satisfying the same nonlinear boundary condition. Now the basic functions ψ_k are $\psi_k(re^{i\theta}) = r^{|k|} \varphi_k$, and then we have the same construction

for Φ as for the exterior domain. Here the surface we have to reach is the one of the complementary of the molten liquid which contains the conductors.

The fact that Ω_1 is simply connected, simplifies even the approach since Φ' always admits an antiderivative. All the results proved in section 3 hold for this problem.

5 Numerical algorithm

5.1 Algorithm for problem P_0

We consider a set of m conductors $(z_i, \alpha_i)_{i=1}^m$, by (2-6) we construct g and for any positive p , problem P_0 is solved by the following procedure

$$\left\{ \begin{array}{l} \text{(a) Find } \varphi^N \text{ solution of (3-10).} \\ \text{(b) Construct } V_N \text{ by (3-12).} \\ \text{(c) Calculate } S_N \text{ by (3-13) and } \Phi_N(z_k) \text{ for } k = 1, \dots, m. \\ \text{(d) Construct the curve } \Gamma = \Phi_N(\Gamma_0). \end{array} \right. \quad (5-1)$$

In the last step we have to test the possible existence of double points for Γ . To solve problem (3-10) a Galerkin spectral method and a fixed-point scheme, introduced in [4] are used. The algorithm for (5-1.a) is

$$\left\{ \begin{array}{l} \varphi^0 \text{ given in } P_N \\ \forall n \geq 0 \text{ then} \\ \quad \bullet \text{ Evaluation of the vector } \vec{f} \text{ of spectral coefficients of the nonlinear} \\ \quad \quad \text{terms : } \tau + \delta\varphi^n - \gamma(\cdot, \varphi^n) \text{ by F.F.T.} \\ \quad \bullet \text{ Solve } \mathcal{A}\vec{\varphi}^{n+1} = \vec{f} \\ \quad \bullet n := n + 1 \end{array} \right.$$

where \mathcal{A} is a $(2N+1)$ matrix defined by $a_{kl} = \langle (\delta + \lambda(\cdot))\varphi_k + C_\varepsilon\varphi_k, \varphi_l \rangle$ and we denote by \vec{u} the vector of Fourier's coefficients of the function u .

At each iteration of the fixed-point scheme, we have to compute the spectral coefficients of the nonlinear term. So it is cheaper to use the Fast Fourier Transform (F.F.T.) to calculate them. The error between the exact spectral coefficients and those obtained by F.F.T. is of the same order than the approximation error (see [3] and [14]). The evaluation of these terms needs only $N \log_2 N$ operations. Moreover the band matrix \mathcal{A}

is hermitian positive definite (see [4]), so the resolution of the linear system is done using a Cholesky factorisation of \mathcal{A} (except if λ is constant, because \mathcal{A} is then, diagonal).

When φ^N is obtained, the second step is to calculate the surface and the image of z_i under Φ_N . The evaluation of $\Phi_N(z)$ by integration of Φ'_N requires the choice of an integration path γ_z such that

$$\Phi_N(z) = c + \int_{\gamma_z} \Phi'_N(\xi) d\xi \quad \forall z \in \overline{\Omega}_0 \quad (5-2)$$

We choose γ_z defined by :

for $z = re^{i\theta}$, first we integrate on the circle $r=1$ from point $A=(1,0)$ to point $B=e^{i\theta}$ and then on the line $s=\theta$ connecting B at z , see Figure 5-1.

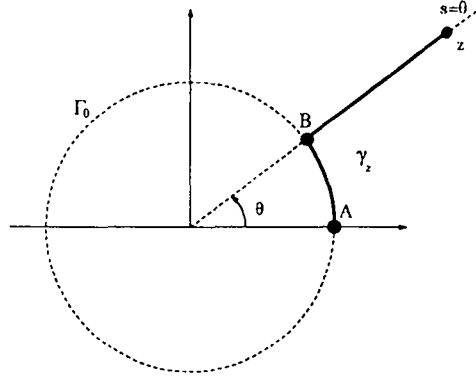


Figure 5-1: path of integration.

By expliciting γ_z in (5-2) we obtain

$$\Phi_N(z) = \Phi_N(1) + i \int_0^\theta e^{i\sigma} \Phi'_N(e^{i\sigma}) d\sigma + e^{i\theta} \int_1^r \Phi'_N(te^{i\theta}) dt \quad (5-3)$$

The two integrals in (5-3) are decomposed into a sum of integrals of length Δl and each integral of length Δl is evaluated by a 6 points Gauss quadrature.

In order to compute S_N we use the procedure described above to evaluate the integral I_N .

5.2 The shaping problem

Our goal here is to obtain a shape for both a given surface S_0 and a given position of the m conductors $(Z_i^0, \alpha_i)_{i=1}^m$. We must adjust the real p and the position of z_i in Ω_0 to reach the wanted configuration. The solution of this problem is obtained by solving the nonlinear equation (2-10).

Let $Y^0 = (S_0, Z_1^0, \dots, Z_m^0)$ the given configuration and G the function defined by

$$\begin{cases} \mathbb{X} \longrightarrow \mathbb{R} \times \mathbb{C}^n \\ x \longmapsto G(x) = Y^0 - F(x) \end{cases} \quad (5-4)$$

Since the evaluation of each partial derivative of F needs the resolution of a linear partial differential equation posed on the exterior of the unit disk, it seemed to us more realistic to consider the secant method to solve (5-4) whose algorithm is

$$\left\{ \begin{array}{l} \text{Let } x^{(0)}, \dots, x^{(m)} \text{ be given, compute } G(x^{(0)}), \dots, G(x^{(m)}). \\ \text{For each } n \geq m \\ \quad \text{i) Construct the two matrices } S^{(n)} \text{ and } D^{(n)} \text{ by} \\ \quad \quad S^{(n)} = [x^{(n)} - x^{(n-1)}, \dots, x^{(n+1-m)} - x^{(n-m)}] \\ \quad \quad D^{(n)} = [G(x^{(n)}) - G(x^{(n-1)}), \dots, G(x^{(n+1-m)}) - G(x^{(n-m)})]. \\ \quad \text{ii) Solve } D^{(n)} \delta x = G(x^{(n)}). \\ \quad \text{iii) Evaluate } x^{(n+1)} = x^{(n)} - S^{(n)} \delta x. \\ \quad \text{iv) Calculate } G(x^{(n+1)}). \end{array} \right. \quad (5-5)$$

The main difficulties we met with this algorithm are the following :

- first, the initialization influences, of course, the convergence. When this initialization turns out to be difficult, we choose a continuation method using known results for great or small τ . Indeed, it is proved in [7] that when τ tends to zero, the conformal mapping converges to the one obtained for $\tau = 0$. But, in this case, computation of Φ is much more easy, see [9], and then we can initialize the algorithm in good conditions. On the other hand when τ is large enough, we can prove that the solution Ω^c is rather closed to a disk. Hence the conformal mapping is near $\Phi(z) = \sqrt{\frac{S_0}{\pi}} z$ and $p \sim \tau \max_{\Gamma_0} C$ which yields

$$x^{(0)} = \left(\tau \sqrt{\frac{\pi}{S_0}}, \sqrt{\frac{\pi}{S_0}} Z_1, \dots, \sqrt{\frac{\pi}{S_0}} Z_m \right).$$

- the second difficulty is due to the domain's definition of the nonlinear function G . We always consider symmetric configurations (Z_i^0, α_i) for which the domain of definition of G is more simple (see part 2), but it remains an open domain \mathbb{H} and algorithm (5-5) may fail since $x^{(n+1)}$ can go out of \mathbb{H} (we can detect this event since the curve Γ has, then, double points). This phenomenon is not so frequent, but it

becomes of course important when we try to reach critical situations (too small τ , too much large surface S_0 with a given configuration of the conductors)

6 Numerical results

For computational purposes the equations and the boundary conditions need to be represented in dimensionless form. The space coordinates are normalized by the radius R of the section, before deformation, of the column of metal, the current density by R^2/I where I is the maximum intensity of the current in the conductors, the magnetic field by $\mu_0 I/R$ and the curvature by R^{-1} . For the convenience of the reader we have used the same symbols for the dimensionless quantities as we have used for the dimensional one in section 2 and after.

The dimensionless system is given by

$$\left\{ \begin{array}{ll} \operatorname{rot} \mathbf{B} = \mathbf{j}_0 & \text{in } \Omega \\ \operatorname{div} \mathbf{B} = 0 & \text{in } \Omega \\ \mathbf{B} \cdot \mathbf{n} = 0 & \text{on } \Gamma \\ \|\mathbf{B}\|^2 + \tau \mathcal{C} = p & \text{on } \Gamma \\ \lim_{\|x\| \rightarrow \infty} \|\mathbf{B}\| = 0 & \end{array} \right. \quad (6-1)$$

where p and $\tau = 2R\sigma/\mu_0 I^2$ are dimensionless numbers.

Let j_0 be given by

$$j_0 = \sum_{k=1}^m \alpha_k \delta_{Z_k} \quad \text{with } \alpha_k \in \mathbb{R}, Z_k \in \Omega \quad (6-2)$$

then g is given by

$$g(\theta) = \sum_{k=1}^m -\frac{\alpha_k}{2\pi} \left\{ \frac{e^{i\theta}}{z_k - e^{i\theta}} + \frac{e^{-i\theta}}{\bar{z}_k - e^{-i\theta}} + 1 \right\} \quad (6-3)$$

where δ_{Z_k} is the Dirac mass at Z_k , Z_k is the adimensional position of the k^{th} conductor, α_k its dimensionless strength and $z_k = \Phi^{-1}(Z_k)$ for $k = 1, \dots, m$. Problem P_0 and equation (2-10) do not change in dimensionless form.

6.1 The P_0 problem

In this section, we present some numerical results when the z_k are given in $\Omega_0 = \Phi^{-1}(\Omega)$ and $p \in \mathbb{R}$. We consider the model problem $z_k = ae^{ik\pi/2}$, $a = 2.0$, and $\alpha_k = (-1)^k$ for $k = 1, \dots, 4$. We choose for the exact solutions those obtained with $N = 150$, and in Table 1 to Table 3 we present the evolution of the error for different values of N . By *Err long* and *Err surf* we mean

$$Err\ long = \max_k \log |\Phi_N(z_k) - \Phi_{150}(z_k)|$$

$$Err\ surf = \log |S_N - S_{150}|.$$

For these different configurations, the solution Ω of P_0 , which is $\Omega = \Phi(\Omega_0)$, is presented in Figure 6-1.

N	4	5	6	8	10	12	15	20
<i>Err long</i>	-1.90	-2.53	-2.91	-3.78	-5.41	-5.89	-8.21	-10.34
<i>Err surf</i>	-1.42	-3.39	-2.38	-3.29	-4.83	-5.39	-8.05	-9.84

Table 1: $\tau = 5 \cdot 10^{-1}$ and $p = 0.55$.

N	4	5	8	9	12	15	20	24
<i>Err long</i>	-0.61	-1.64	-2.68	-4.08	-4.81	-6.98	-9.28	-11.56
<i>Err surf</i>	-0.14	-1.75	-2.21	-4.09	-4.36	-6.42	-8.84	-11.13

Table 2: $\tau = 5 \cdot 10^{-2}$, and $p = 0.10$.

N	12	15	20	24	30	40	50	60	80	100
<i>Err long</i>	-1.81	-2.24	-2.69	-3.08	-3.45	-4.76	-5.75	-7.02	-9.35	-11.71
<i>Err surf</i>	-1.21	-1.55	-2.08	-2.47	-2.84	-4.16	-5.15	-6.42	-8.75	-11.11

Table 3: $\tau = 1 \cdot 10^{-3}$ and $p = 0.03$.

These tables show that, when τ is smaller, the decay of the error is slower. In the last case, as we can guess in view of the Figure 6-1 (c), the strip of analyticity η , see (3-17), is smaller than in the other cases. In this first example a good agreement with Theorem 3-3 is therefore observed.

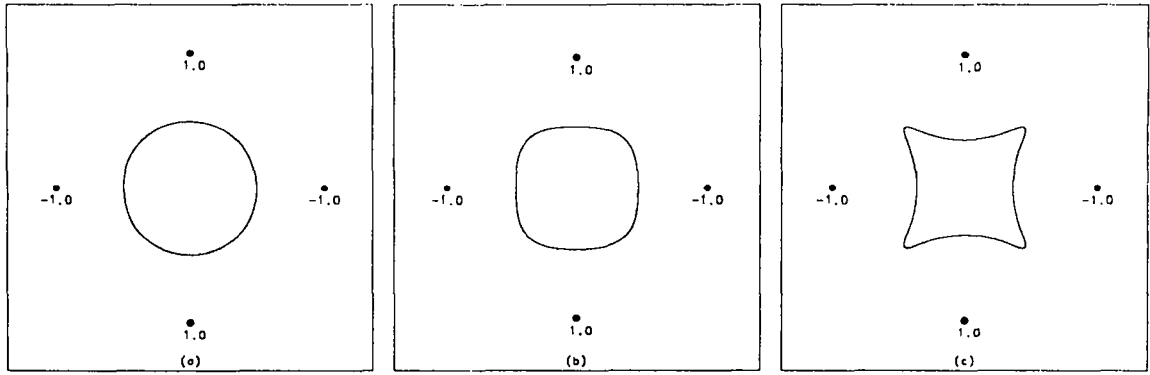


Figure 6-1: (a) $\tau = 1 \cdot 10^{-1}$; (b) $\tau = 5 \cdot 10^{-2}$ and (c) $\tau = 1 \cdot 10^{-3}$.

We present in Table 4 and Figure 6-2 below, different kinds of shape for various positions of conductors and density currents.

τ	m	z_k	p	length	Surf.	N	Figure 6-2
$1.0 \cdot 10^{-3}$	4	$1.2 e^{\frac{\pi}{4}i+k\frac{\pi}{2}}$	0.2	1.19	0.989	50	(a)
$1.0 \cdot 10^{-3}$	4	$1.5 e^{\frac{\pi}{2}ik}$	0.1	0.894	1.115	40	(b)
$1.0 \cdot 10^{-1}$	3	$2.0 e^{\frac{2\pi}{3}ik}$	0.25	0.873	1.539	40	(c)

Table 4:

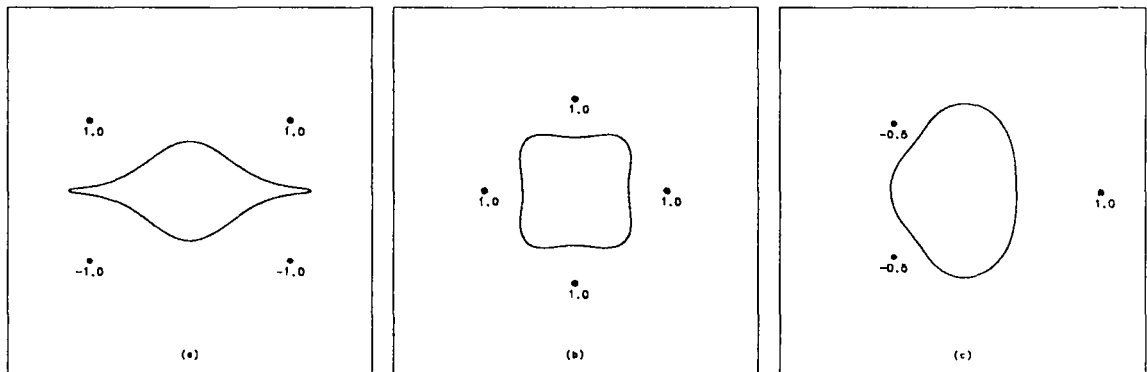


Figure 6-2: Image of Ω_0 under Φ .

Finally in Table 5 and Figure 6-3 some simple configurations for the interior shaping problem are shown.

τ	m	z_k	p	length	Surf.	N	Figure 6-3
$1.0 \cdot 10^{-3}$	3	$0.5e^{\frac{2\pi}{3}ik}$	0.45	0.354	1.57	40	(a)
$1.0 \cdot 10^{-3}$	3	$0.5e^{\frac{2\pi}{3}ik}$	0.45	0.495	2.79	40	(b)
$1.0 \cdot 10^{-3}$	4	$0.5e^{\frac{\pi}{2}ik}$	0.15	0.517	2.02	40	(c)

Table 5:

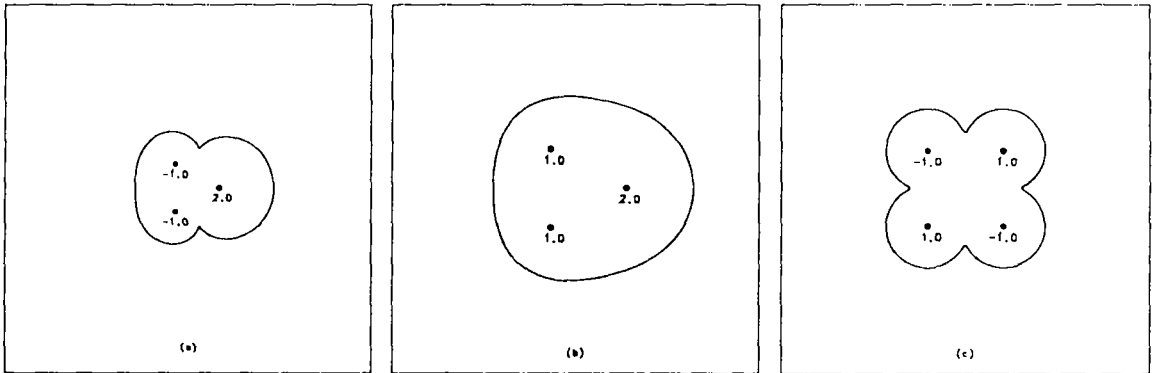


Figure 6-3: Image of Ω_1 under Φ .

6.2 The shaping problem

Now we consider a given position of the conductors in Ω and we have to reach the dimensionless surface which is $S = \pi$. We present some results for both the exterior and interior problem. The wanted configuration is reached when $|G(x^{n+1})| \leq 5 \cdot 10^{-7}$.

6.2.1 The exterior shaping

First of all, we compare our results with those obtained by Deframond see [6] in the classical quadrupole-like field produced by four conductors, see also [13]. Their approach is based on the minimization of the energy and the introduction of conformal map in order to compute shape derivatives. In this case the magnetic field is produced by four vertical conductors located at $Z_k = le^{ik\pi/2}$ with intensity $\alpha_k = (-1)^k$ for $k = 1$ to 4. We present in Table 6 for two lengths l and for several values of τ the elongation of the form which is $el = |\Phi(e^{i\pi/4}) - \text{centre}|$ in our case, where *centre* is the centre of the image by

Φ of the solution z_k of (2-10) and el_* is the elongation obtained by [6]. Table 6 shows a very good agreement between the results of the two methods

$\pi\tau/2$	l=1.7		l=1.9	
	el	el_*	el	el_*
0.1	1.083	1.08	1.056	1.06
0.05	1.137	1.13	1.096	1.09
0.025	1.213	1.21	1.154	1.15
0.02			1.177	1.18

Table 6: Elongation comparison for the four conductors case.

In the same way, Pierre and Roche [12] obtained the same kind of shape using a boundary element method coupled with an optimization of the energy. The advantage of the latter method is that it can be applied for the 3-dimensions problem (the so-called levitation problem). Here we obtain very accurate results since we do use the analyticity of the curve by a good spectral approximation of the conformal map, see theorem 3.3. Moreover our method may reach positions with very small values of τ .

In the Table 7 and in the Figure 6-4, we present some shapes obtained by the complete algorithm including the resolution of (2-10). In these cases, due to the symmetries of the conductors we only have to adjust one length and the parameter p . With a good initialization (see above) the complete algorithm needs to call the previous P_0 algorithm less than ten times to reach the good location of the conductors.

τ	m	Z_k	p	z_k	N	Figure 6-4
$5.0 \cdot 10^{-2}$	2	$1.2e^{ik\pi}$	0.093	$1.41e^{ik\pi}$	40	(a)
$1.0 \cdot 10^{-2}$	4	$2.0e^{\frac{2\pi}{3}ik}$	0.215	$2.0e^{\frac{2\pi}{3}ik}$	80	(b)
$9.0 \cdot 10^{-3}$	8	$1.5e^{\frac{\pi}{4}ik}$	0.208	$1.5e^{\frac{\pi}{4}ik}$	40	(c)

Table 7:

Now we present more complex configurations of conductors. In the following cases, we have to adjust two lengths and the parameter p .

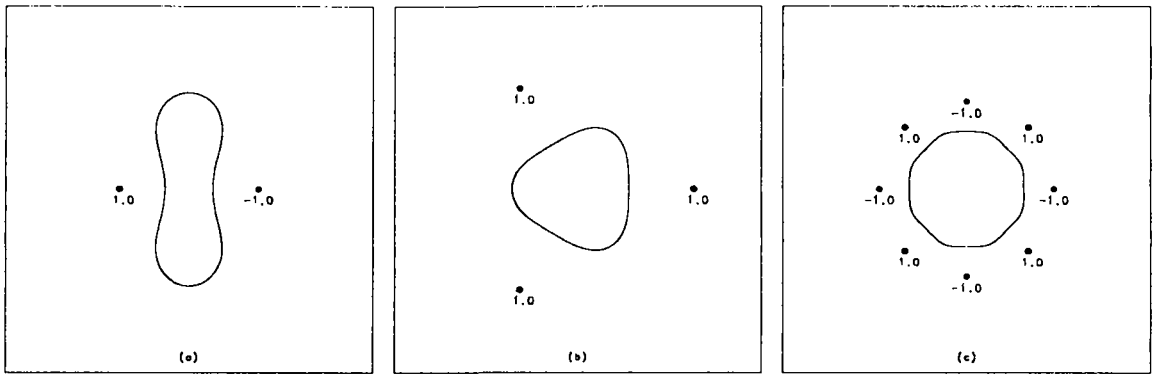


Figure 6-4: Image of Ω_0 under Φ .

τ	m	Z_k	ρ	z_k	N	Figure 6-4
$5.0 \cdot 10^{-2}$	4	$\begin{cases} 1.5 e^{\pi i k}, & k = 0, 1 \\ 2.5 e^{\pi i k}, & k = 0, 1 \end{cases}$	0.064	$\begin{cases} 1.5 e^{\pi i k}, & k = 0, 1 \\ 2.0 e^{\pi i k}, & k = 0, 1 \end{cases}$	40	(a)
$5.0 \cdot 10^{-3}$	8	$\begin{cases} 1.5 e^{\frac{\pi}{2} i k}, & k = 0, 3 \\ 2.5 e^{\frac{\pi}{2} i k}, & k = 0, 3 \end{cases}$	0.021	$\begin{cases} 1.60 e^{\frac{\pi}{2} i k}, & k = 0, 3 \\ 2.53 e^{\frac{\pi}{2} i k}, & k = 0, 3 \end{cases}$	60	(b)
$1.0 \cdot 10^{-2}$	4	$(\pm 1.3, \pm 0.9)$	0.033	$(\pm 1.17, \pm 0.82)$	80	(b)

Table 8:

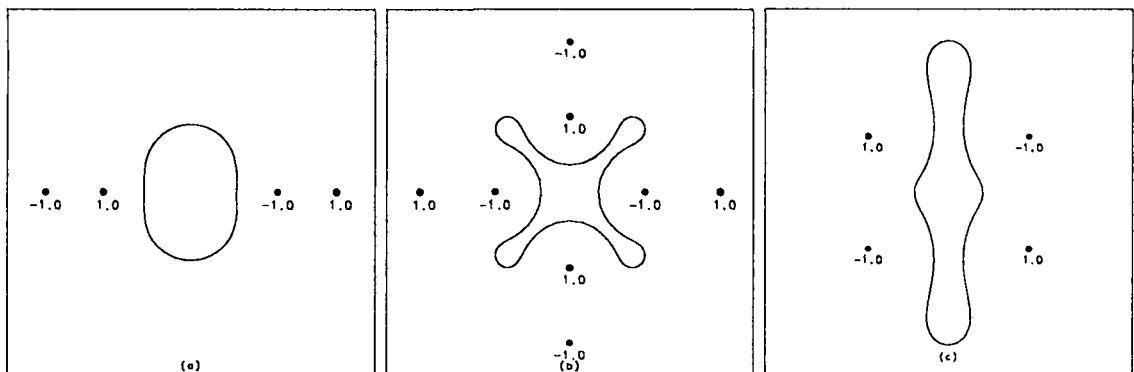


Figure 6-5: Image of Ω_0 under Φ .

Coming back to the four conductors case, Henrot and Pierre in [9] present a complete study for P_0 problem when $\tau = 0$. In this case they have obtained an analytic solution for Φ . Moreover if l is the distance between the conductors and the origin, they show that for $\pi l^{-2} < c \sim 0.624$, there exists a conformal map and then a solution for the shaping problem. For $l = 2.5$, we present in Table 9 the number of nodes N needed to obtain convergence, the elongation of the form and (a,p) the solution of (2-10). The values for $\tau = 0$ are obtained by the analytic expression of Φ , S , and l given in [9].

τ	N	el	a	p
1.0	9	1.001	2.500	1.02
$2.25 \cdot 10^{-2}$	15	1.051	2.494	$4.15 \cdot 10^{-2}$
$1.00 \cdot 10^{-2}$	15	1.094	2.478	$2.80 \cdot 10^{-2}$
$5.00 \cdot 10^{-3}$	15	1.150	2.448	$2.20 \cdot 10^{-2}$
$1.00 \cdot 10^{-3}$	36	1.332	2.310	$1.62 \cdot 10^{-2}$
$5.00 \cdot 10^{-4}$	48	1.418	2.238	$1.53 \cdot 10^{-2}$
$1.00 \cdot 10^{-4}$	100	1.589	2.097	$1.45 \cdot 10^{-2}$
$5.00 \cdot 10^{-6}$	162	1.752	1.972	$1.43 \cdot 10^{-2}$
0.		1.790	1.949	$1.40 \cdot 10^{-2}$

Table 9: Evolution of N , a and p when τ tends to 0.

As we can see in Figure 6-6, when τ tends to 0 the variations of the derivatives of Φ become very important, and then the strip of analyticity of the function g^2 (see (3-17)) decreases which explains the greater number of nodes needed to obtain a good approximation, see Table 9 and theorem 3.3. We obtain exactly the same kind of shape, when τ tends to 0, to those presented by Shercliff in [13].

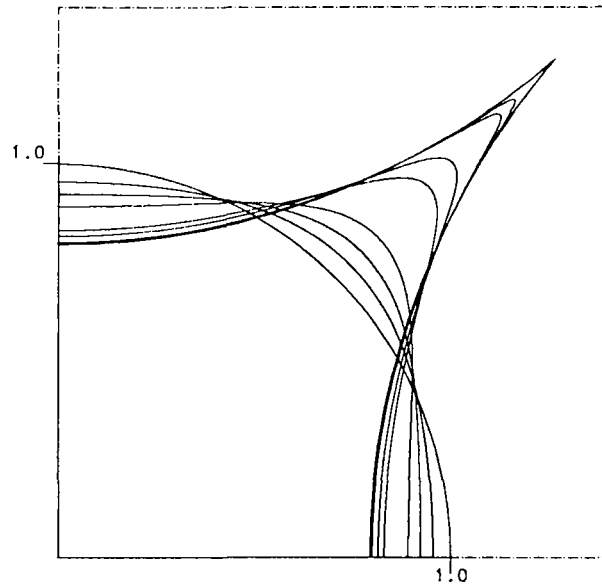


Figure 6-6: τ tends to 0, for $l=2.5$.

6.2.2 The interior shaping

In this section we present briefly three configurations of conductors. In the interior shaping we must reach the surface $S = \pi$ which represent the volume without liquid. We can observe in Table 10 that we need less points for small values of τ than for the exterior problem to obtain the solution.

τ	m	Z_k	p	z_k	N	Figure 6-7
$5.0 \cdot 10^{-5}$	2	$1.2 e^{ik\pi}$	0.036	$0.506 e^{ik\pi}$	30	(a)
$5.0 \cdot 10^{-3}$	4	$0.7 e^{\frac{\pi}{2}ik}$	0.130	$0.701 e^{\frac{\pi}{2}ik}$	25	(b)
$5.0 \cdot 10^{-3}$	5	$\begin{cases} 0.703 e^{\frac{\pi}{2}ik}, k = 0, 3 \\ 3.3 \cdot 10^{-3} \end{cases}$	$3.1 \cdot 10^{-3}$	$\begin{cases} 0.7 e^{\frac{\pi}{2}ik}, k = 0, 3 \\ 0.0 \end{cases}$	30	(c)

Table 10:

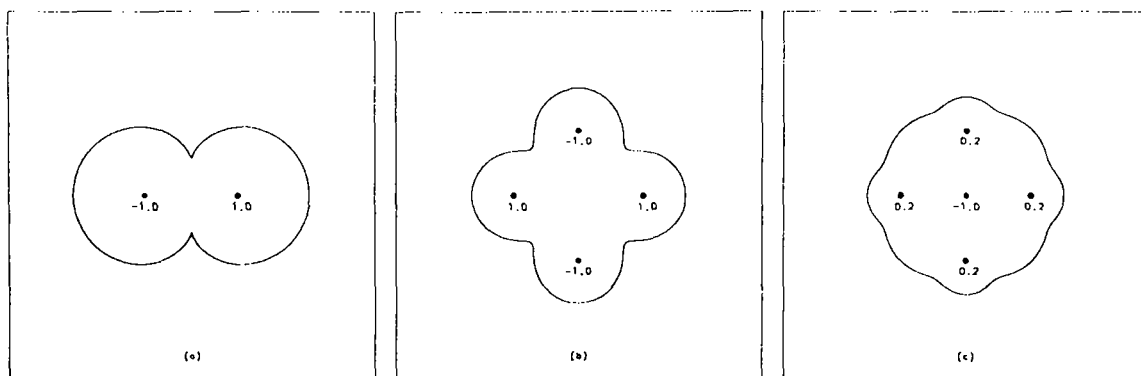


Figure 6-7: Image of Ω_1 under Φ .

References

- [1] J.P. Boyd. *Chebyshev, Fourier Spectrals Methods*, volume 49 of *Lecture Notes in Engineering*. Springer-Verlag, New-York, 1989.
- [2] J.P. Brancher, J. Etay, and O. Sero-Guillaume. Formage d'une lame. *J.M.T.A.*, 2(6):976–989, 1983.
- [3] C. Canuto, M.Y. Hussaini, A. Quarteroni, and T.A. Zang. *Spectral methods in fluid dynamics*. Springer-Verlag, New-York, 1987.
- [4] O. Coulaud and A. Henrot. A nonlinear boundary value problem solved by spectral methods. *Applicable Analysis*, 43:229–244, 1991.
- [5] R. Dautray and J.L. Lions. *Analyse mathématique et calcul numérique pour les sciences et les techniques*, volume 1. Masson Paris, 1984.
- [6] Deframond. *Quelques aspects du formage électromagnétique des surfaces libres. Application et hydrodynamique*. PhD thesis, INPG, 1985.
- [7] A. Henrot. Behaviour of the free boundary in electromagnetic shaping when the surface tension vanishes. *To appear in Nonlinear Analysis*.

- [8] A. Henrot. Injectivité globale d'une fonction holomorphe définie sur un domaine extérieur. *Private communication*, 1991.
- [9] A. Henrot and M. Pierre. About existence of a free boundary in electromagnetic shaping. In *Recent advances in nonlinear elliptic and parabolic problems*, volume 208, pages 283–293. Pitman Research Notes Series, 1989.
- [10] A. Henrot and M. Pierre. Un problème inverse en formage des métaux liquides. *M²AN*, 23:155–177, 1989.
- [11] A. Henrot and M. Pierre. About existence of equilibria in electromagnetic casting. *Quarterly of Applied Mathematics*, XLIX(3):563–575, September 1991.
- [12] M. Pierre and J.R. Roche. Computation of free surfaces in the electromagnetic shaping of liquid metals by optimization algorithms. *European Journal of mechanics, B/Fluids*, 10(5):489–500, 1991.
- [13] J.A. Shercliff. Magnetic shaping of molten metal columns. *Proc. Royal. Soc. London*, 375(A):455–473, 1981.
- [14] E. Tadmor. The exponential accuracy of Fourier and Chebyshev differencing methods. *SIAM J. Numer. Anal.*, 23, February 1986.

ISSN 0249 - 6399